FISEVIER

Contents lists available at ScienceDirect

International Journal of Biological Macromolecules

journal homepage: www.elsevier.com/locate/ijbiomac





Cloning, expression and functional characterization of recombinant tumor necrosis factor $\alpha 1$ (TNF $\alpha 1$) from white crucian carp in gut immune regulation

Shi-Yun Li ^a, Ning-Xia Xiong ^{a, b}, Ke-Xin Li ^a, Jin-Fang Huang ^a, Jie Ou ^a, Fei Wang ^a, Ming-Zhu Huang ^c, Sheng-Wei Luo ^{a, *}

- a State Key Laboratory of Developmental Biology of Freshwater Fish, College of Life Science, Hunan Normal University, Changsha 410081, PR China
- ^b Department of Aquatic Animal Medicine, College of Fisheries, Huazhong Agricultural University, Wuhan 430070, PR China

ARTICLE INFO

Keywords: Crucian carp TNF α Antioxidant Immune regulation

ABSTRACT

TNF α is one of important cytokines belonging to TNF superfamily, which can exhibit a pleiotropic effect in immune modulation, homeostasis as well as pathogenesis. However, its immunoregulatory function on mucosal immunity in fish gut are still unclear. In this study, we aimed to investigated the immunoregulatory role of TNF α 1 in midgut of white crucian carp (WCC). WCC-TNF α 1 sequence and its deduced structure were firstly identified in WCC. Then, tissue-specific analysis revealed that high-level WCC-TNF α 1 expression was detected in gill. After *Aeromonas hydrophila* and lipopolysaccharide (LPS) stimulated, increased trends of WCC-TNF α 1 expressions were detected in immune-related tissues and cultured fish cells, respectively. WCC anal-intubated with WCC-TNF α 1 fusion protein showed the increased levels of edema and fuzzy appearance in impaired villi, along with atrophy and reduction of goblet cells (GC). Moreover, the expression levels of tight junction (TJ) genes and mucin genes were consistently lower than those of the control (P < 0.05). WCC-TNF α 1 treatment could sharply decrease antioxidant status in midgut, while the expression levels of caspase (CASP) genes, unfolded protein response (UPR) genes and redox response genes increased dramatically. Our results suggested that WCC-TNF α 1 could exhibit a detrimental effect on antioxidant and mucosal immune regulation in midgut of WCC.

1. Introduction

Water contamination can promote the increased levels of infectious agents in aquatic environment, exhibiting a high immunotoxicity in aqueous livings [1]. Pollutants, including antibiotics and heavy metals, can show a detrimental influence on intracellular homeostasis and immune regulation in teleost fish [2]. Although immunoprophylaxis can increase fish immunity against infectious diseases, pollutant bio-accumulation can enable rapid occurrence of pathogenic bacteria with multiple resistance and high virulence by challenging the microbe community in water environment [3,4]. Emerging evidences suggest that pathogenic diseases can pose a huge threat to the health of farmed fish, leading to a great economic loss in aquaculture [5]. Whist invading pathogens succeed in breaching mucosal barriers of teleost fish, they instantly orchestrate host immune response and exacerbate the degrees of acute infectious diseases [6]. Crucian carp (Carassius auratus) is an

important farmed fish species in China, but its farming process suffers from pathogenic infection [7]. As known pathogenic bacteria, *Aeromonas hydrophila* can increase fish morbidity by generating toxins [8]. Our previous studies indicated that *A. hydrophila* can disturb epithelial permeability in midgut, increase bacterial burdens as well as dysregulate immune response in gut-liver axis of WCC [9].

Biotic or abiotic stressors may exhibit suppressive effects on fish immunity and then render fish more susceptible to invading pathogens [10], but teleost fish possess large quantities of immune-related properties such as pathogen recognition receptors (PRRs) and complement cascades, which play crucial roles in the front line of pathogenic recognition and elimination [11]. The reciprocal interaction of gut, gut flora and liver constitute an immune microenvironment in gut-liver axis, which has been gradually recognized in teleost fish [12,13]. Gut-associated lymphoid tissue (GALT) is playing an predominant role in mucosal immune regulation in fish [14], whereas gut mucosal surface

^c National R&D center for freshwater fish processing, Jiangxi Normal University, Nanchang 330022, China

^{*} Corresponding author at: College of Life Science, Hunan Normal University, Changsha 410081, PR China. *E-mail addresses*: swluo@hunnu.edu.cn, swluo1@163.com (S.-W. Luo).

acting as biophysical barrier can promote mucus secretion, increase immune surveillance as well as participate in pathogenic elimination [15,16]. Current studies suggest that immune-regulated signals, including cytokine secretion, pathogenic recognition as well as immune cell activation, can exhibit synergistic effects on immune regulation of gut-liver axis in fish [17,18]. Among known immune effectors, TNF α is a glycopeptide hormone that can exert a pleiotropic role in immune activation, inflammatory response and apoptotic processes [19]. Recent findings suggest that teleost fish possess most of TNF genes and their receptors found in mammals and some homologues exclusively present in teleost fish, but OX40 ligand (TNFSF4), CD27 ligand (TNFSF7), CD30 ligand (TNFSF8) and their cognate receptors are absent [20]. $TNF\alpha$ function has been extensively studied in mammals, but the regulatory role of TNF α in teleost fish may require further study. Some teleost fish may possess two types of TNF α homologues that located on two separate chromosomes [21]. Most studies focus on gene structure and expression analysis of TNFα in teleost fish, such as large yellow croaker [22], rainbow trout [23] and tilapia [24]. However, the immunoregulatory role of TNFα1 in gut barrier function in WCC was unclear.

Therefore, current study aimed to characterize architectures of TNF α 1 in WCC. Then, the expression profiles of WCC-TNF α 1 were measured in immune-related tissues or cultured fish fibroblast cell lines upon stimulation. After that, WCCs received the gut perfusion with WCC-TNF α 1 fusion protein in order to investigate its immunoregulatory function on mucosal immune response in midgut, which may provide a new insight into the regulatory function of TNF α 1 in WCC.

2. Materials and methods

2.1. Ethics approval

All applicable international, national, and/or institutional guidelines for the care and use of animals were followed. We followed the laboratory animal guideline for the ethical review of the animal welfare of China (GB/T 35892–2018).

2.2. Animals

Healthy WCCs were obtained from a fishing base in Changsha, China. Then, fish (approximately 16.61 \pm 1.95 g) were acclimatized in aquarium and fed with diet twice daily till 24 h before the subsequent experiment. Water quality was controlled to prevent the emergence of infectious diseases by daily removing the excess of fish feed and feces.

2.3. Fish infected with A. hydrophila

A. hydrophila L3–3 strain (NCBI accession number: OM184261) was isolated from liver of the dying crucian carp [25]. A. hydrophila L3–3 strain was cultured in Luria-Bertani (LB) medium at 30 °C for 24 h and then resuspended in 1 \times PBS (pH 7.3) before use [26]. Intraperitoneal injection of A. hydrophila (1× 10^7 CFU mL $^{-1}$) was used as A. hydrophila challenge group, while fish receiving the injection of equivalent volume of sterile PBS was used as control group. Tissues were isolated at 0, 6, 12, 24, 36 and 48 h post-injection, immediately frozen in liquid nitrogen and preserved in -80 °C. Each group contained three biological replicates, respectively.

2.4. Cell culture and LPS stimulation

WCC fibroblast cells (WCCFCs) were cultured in dulbecco's modified eagle medium (DMEM, Gibco, USA) supplemented with 10 % fetal bovine serum (FBS, Gibco, USA) at 26 °C with a humidified atmosphere of 5 % CO₂ as described previously [27]. Then, WCCFCs were seeded into 6-well plates at 80 % confluence for 24 h. Then, cultured medium (DMEM, 10%FBS) was replaced with fresh medium containing 500 ng/mL of LPS (*Escherichia coli* O111:B4, Sigma, USA) [28]. Cells were

harvested at 0, 6, 12, 24, 36 and 48 h post-treatment, frozen in liquid nitrogen and preserved in $-80\ ^{\circ}\text{C}.$

2.5. Gene cloning, bioinformatics analysis and plasmid construction

Based on previous studies, open reading frame (ORF) sequence of WCC-TNF α 1 was cloned [29]. After that, domain structure and binding sites were analyzed by NCBI blast program [30]. Then, tertiary structure was generated by phyre2 program and phylogenetic tree analysis was constructed by using MEGA 6.0 software and ITOL program. Moreover, ORF sequence was ligated to pET32 α and pcDNA3.1 plasmid, respectively. The constructed vectors were transformed into *Escherichia coli* and positive bacterial clone was subjected to sequence confirmation (Tsingke, Beijing, China).

2.6. Dual-luciferase reporter assay

Dual-luciferase reporter assay was performed in fish cells as previously described [31,32]. Briefly, WCCFCs were seeded in 24-well plates overnight. Then, cell were co-transfected with various amount of recombinant vector pcDNA3.1, pcDNA3.1-WCC-TNF α 1, PRL-TK and NF- κ B Luc to investigate transcriptional activity of NF- κ B reporter. Furthermore, transfected cells were stimulated with LPS at 200 ng/mL for 6 h. Following 24 h, luciferase activity were analyzed by using a dual-luciferase reporter assay system (Promega). Relative folds of luciferase activity were normalized to the level of renilla luciferase. The results were repeated in triplicate.

2.7. Prokaryotic expression, purification and validation of $TNF\alpha 1$

In vitro production and purification of fusion protein were performed as described previously [33]. The plasmid pET32 α and pET32 α -WCC-TNFα1 were transformed into *E. coli* BL21 clone and then positive clones were cultured in LB medium until OD_{600} value reached about 0.6. Following 4 h incubation with 1 mM Isopropyl β-D-thiogalactoside (IPTG, Sangon Biotech, China), bacteria were sonicated and dissolved in urea-containing buffer. After that, supernatant proteins were purified by using Ni-NTA Sefinose(TM) Resin 6FF (Sangon Biotech, China). In brief, Ni-NTA His bind resin was loaded with $1 \times$ binding buffer, Ni ion solution, $1 \times$ binding buffer, soluble recombinant protein solution, $1 \times$ binding buffer, 1 \times wash buffer and 1 \times elution buffer, respectively. Then, the released soluble WCC-TNFα1 protein was subjected to continuous protein refolding process. Protein refolding assay was performed at 4 °C by using dialysate containing gradient-decreased urea content. Purified WCC-TNFα1 protein was separated by SDS-PAGE and validated by western-blotting. After incubation with HIS-tag primary antibody and alkaline phosphatase (AP)-conjugated secondary antibody, PVDF membrane were visualized.

2.8. Gut perfusion with $TNF\alpha 1$ fusion protein

Gut perfusion assay was performed as described previously [34]. Briefly, fish were anally intubated with TNF α 1 fusion protein (0.15 mg/per fish) by using a gavage needle inserted into a depth of approximately 3 cm, while equivalent per gram of pET32 α tag perfusion was used as control group, respectively. Tissues were isolated at 48 h post-perfusion, then immediately frozen in liquid nitrogen and preserved in $-80~^{\circ}$ C. Each group contained three biological replicates, respectively.

2.9. Histological analysis

The isolated midgut samples were fixed in bouin solution, dehydrated in ethanol, clarified in xylene and then embedded in paraffin wax. Then, paraffin-embedded samples were sectioned and stained according to the protocol of a periodic acid-schiff (PAS) staining kit (Solarbio, China) [35]. Microstructures of midgut tissues were observed

Table 1
The primer sequences used in this study.

Primer names	Sequence direction $(5' \rightarrow 3')$	Use
ΤΝΓα1-Γ	ATGATGGATCTTGAGAGTCAGCT	clone
TNFα1-R	TCATAAAGCAAACACCCCGAA	clone
pet-TNFα1-F	CCGGAATTCATGCTCAACAAGTCTCAGAA	vector
pet-TNFα1-R	CCGCTCGAGTTAATGATGATGATGATGTAAAGCAAACACCCCGAAGA	vector
RT-18S-F	CGGAGGTTCGAAGACGATCA	qPCR
RT-18S-R	GAGGTTTCCCGTGTTGAGTC	qPCR
RT-TNFα1-F	TGTGGGGTCCTGCTGGC	qPCR
RT-TNFα1-R	TTCCTGATTGTTCTGAGACTTGTTG	qPCR
RT-FADD-F	TTGTGCCAAGAAGAAGTCGG	qPCR
RT-FADD -R	TGTTTTCGCAGGAGTTCAGTG	qPCR
RT-CASP7-F	CTAAGCCACGGCGAGGA	qPCR
RT- CASP7-R	CGGAACCCCGACAAGC	qPCR
RT-CASP3-F	AGATGCTGCTGAGGTCGGG	qPCR
RT-CASP3-R	GGTCACCACGGCAACTG	qPCR
RT-CASP8-F	TGTGAATCTTCCAAAGGCAAA	qPCR
RT-CASP8-R	CTGTATCCGCAACAACCGAG	qPCR
RT-HSP70-F	ACGAGGCAGTGGCTTATGG	qPCR
RT-HSP70-R	GGGTCTGTTTGGTGGGGAT	qPCR
RT-HSP90α-F	AGCAGCCGATGATGGA	qPCR
RT-HSP90α-R	GGATTTGGCGATGGTTC	qPCR
RT-HSP90β-F	TGGGATTGGGGATTGATGA	qPCR
RT-HSP90β-R	CCTTCCAGAGGTGGGATTTC	qPCR
·	CCTGGACTCACTTCCGTTCG	qPCR
RT-ATF4-F RT-ATF4-R	GCTGCCGTTTTGTTCTGCT	_
		qPCR
RT-ATF6-F	TCTGTGATGAAAGCAACGC	qPCR
RT-ATF6-R	CAGGGGAAGGAAAGATTCT	qPCR
RT-IRE1-F	AGCGGCAAGCATCCTCCTCT	qPCR
RT-IRE1-R	CCACCATCCGTCCTCT	qPCR
RT-PDIA3-F	CTGAGCCTGTTCCAGAGTCCA	qPCR
RT- PDIA3-R	TCCAGAGGGCACAAAGTAAATG	qPCR
RT-XBP1-F	TCCACTTTGACCACACTCTACACC	qPCR
RT-XBP1-R	TTCATCTTTGACGGACACCATT	qPCR
RT-ZO-1-F	TGCCCAGAGGTGAAGAGGTC	qPCR
RT- ZO-1-R	GCCCAGTTTGCCGTTGTAA	qPCR
RT-occludin -F	GTTGCCCATCCGTAGTTCAGT	qPCR
RT-occludin -R	CTTCAGCCAGACGCTTGTTG	qPCR
RT-claudin-1-F	GCTCCTCGGATACTCTTTGGC	qPCR
RT-claudin-1-R	TTTCATCAGACAGACAGGTGGTG	qPCR
RT-claudin-3-F	GTCAATGGGAATGGG	qPCR
RT-claudin-3-R	AAGCCTGAAGGTCTTGCGATA	qPCR
RT-claudin-6-F	GACCATCGCTGTTCCAAGA	qPCR
RT-claudin-6-R	ATTCCATCCACAAGCCCTC	qPCR
RT-claudin-9-F	GGCAAACACGGGTCTTCAG	qPCR
RT-claudin-9-R	CGGTGCGGCGACATTC	qPCR
RT-MUC2-F	CCTGACATTTTGTGGTGGAGA	qPCR
RT-MUC2-R	CTGTGCGATTACTTGAGCGAG	qPCR
RT-MUC13-F	TGCCACATCAGTTTCAGTTGC	qPCR
RT-MUC13-R	TTCACCCACCGCCATTTC	qPCR
RT-COX4-F	ACAACAACCGTCTGGATACACC	qPCR
RT-COX4-R	CTCTTTGGAACCTTGCCTCAT	qPCR
RT-OXR1-F	CATCAGGCAGCATTAGAGGC	qPCR
RT-OXR1-R	TGGAGGGGATTTTAGGTTTTG	qPCR
RT-TrxR-F	TCCTGGGGTCTGGGTGG	qPCR
RT-TrxR-R	CAGCCGAACTTGCGTGC	qPCR
RT-CYP11A1-F	CTGAGGGTCATTATCCCAAGAG	qPCR
RT-CYP11A1-R	TGAGCAGGACGCCGTATTT	qPCR
RT-TXNL1-F	TGATGCCGTTCGTCAGTAAAG	qPCR
		-

by using a light microscope with $200\times$ magnification. The average changes of goblet cell (GC) numbers and villus length-to-width (L/W) ratios were calculated. The experiment was repeated in triplicate.

2.10. Detection of biochemistry change

2.10.1. Catalase (CAT) activity

According to previous studies, the above fusion protein treated midgut samples were homogenized on ice and the protein concentration was quantified by bicinchoninic acid (BCA) method [36]. Then, CAT activities in midgut were measured at OD_{405} absorbance by using a CAT activity kit (Nanjing Jiancheng Bioengineering Institute, China). Results were given in units of CAT activity per milligram of protein, where 1 U of

CAT is defined as the amount of enzyme decomposing 1 $\mu mol\ H_2O_2$ per second. The experiment was repeated in triplicate.

2.10.2. Glutathione peroxidase (GPx) activity

GPx activities in midgut were observed at OD_{340} absorbance by using a GPx activity kit (Beyotime Biotechnology, China). Results were shown as U GPx activity per milligram of protein. The experiment was repeated in triplicate.

2.10.3. Total superoxide dismutase (SOD) activity

Total SOD activity in midgut were detected at OD_{560} absorbance by using a total SOD activity kit (Beyotime Biotechnology, Shanghai, China). Results were given in units of SOD activity per milligram of

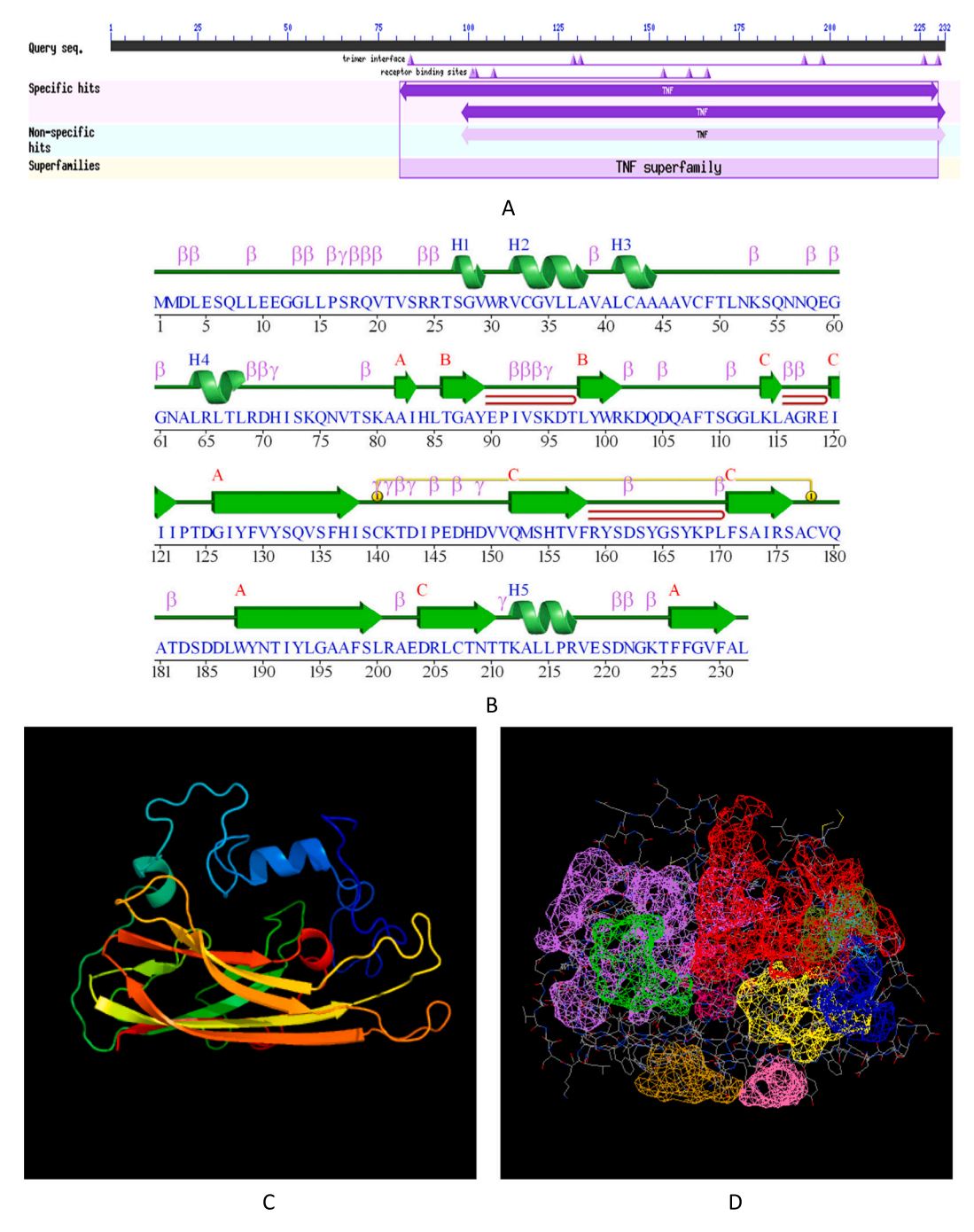


Fig. 1. Bioinformatics analysis of WCC-TNFα1. (A) WCC-TNFα1 amino acid sequence analyzed by NCBI. (B) Secondary structure prediction of WCC-TNFα1. (C) Helix strand, Helices labeled: H1, H2, ... and strands by their sheets A, B, ...; β: beta turn; γ: gamma turn; beta hairpin; is disulphide bond. (C) Tertiary structure prediction. Structures were colored by rainbow from N to C terminus. (D) Cleft domain prediction in tertiary structure of WCC-TNFα1. Cleft domains were colored by rainbow.

protein, where 1 U of SOD is defined as the amount of enzyme producing 50 % inhibition of SOD. The experiment was repeated in triplicate.

2.10.4. NADPH/NADP+ ratio

NADPH/NADP $^+$ contents in midgut were determined by using NADPH/NADP $^+$ assay kit (Beyotime Biotechnology, Shanghai, China). Then, NADPH/NADP $^+$ ratios were calculated as: [NADPH]/[NADP $^+$] = [NADPH]/([NADP total]-[NADPH]). The experiment was repeated in triplicate.

2.10.5. Determination of relative reactive oxygen species (ROS) production ROS levels in supernatants of 10 % midgut homogenates were measured by DCFH-DA probe (Beyotime Biotechnology, Shanghai, China). After triplicate repeats, ROS contents were calculated with absorbance changes at excitation/emission wavelength of OD_{480/520} nm.

2.10.6. Malondialdehyde (MDA) amounts

Free MDA and lipid hydroperoxides can be determined by thio-barbituric acid (TBA) method. According to protocols of lipid peroxidation MDA assay kit (Beyotime Biotechnology, Shanghai, China), midgut MDA amount was measured. The concentration of MDA was

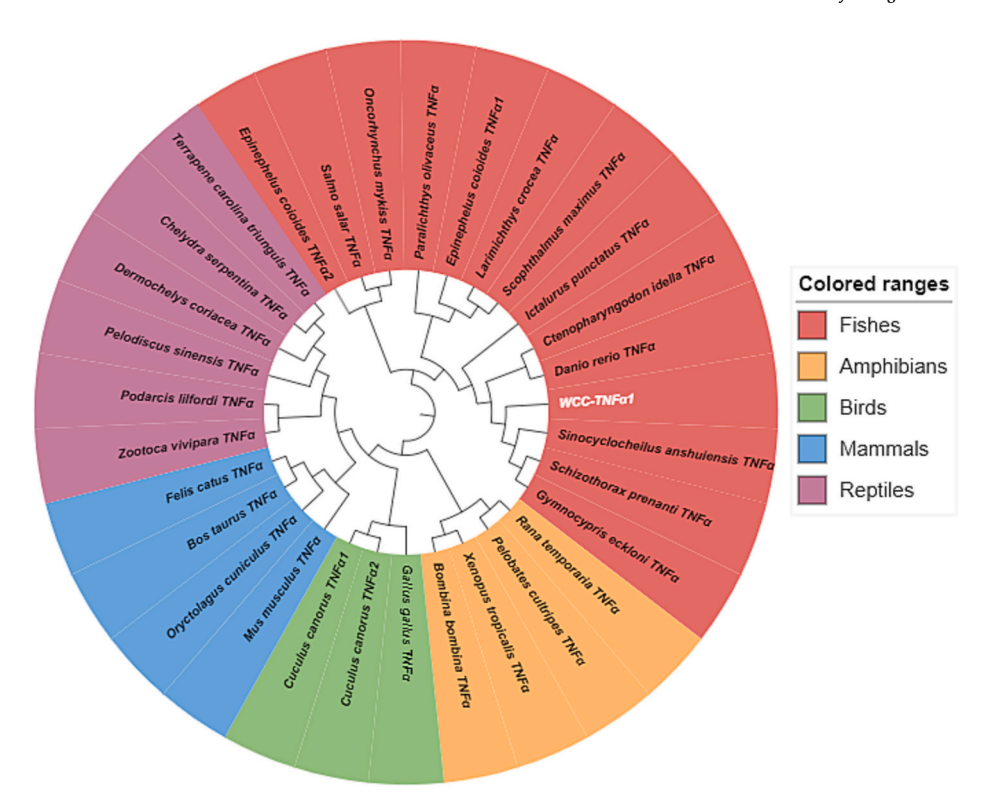


Fig. 2. Phylogenetic tree analysis by using NJ method with 1000 bootstrap replications. The amino acid sequences used in this study were shown below: Felis catus TNFα1, NP_001009835.1; Mus musculus TNFα, AAC82484.1; Bos taurus TNFα, NP_776391.2; Oryctolagus cuniculus TNFα, NP_001075732.1; Zootoca vivipara TNFα, XP_034954640.1; Terrapene carolina triunguis TNFα, XP_029770241.1; Chelydra serpentine TNFα, KAG6921425.1; Dermochelys coriacea TNFα, XP_038227681.1; Pelobates cultripes TNFα, CAH2314388.1; Pelodiscus sinensis TNFα, XP_014431445.1; Podarcis lilfordi TNFα, CAI5768086.1; Cuculus canorus TNFα1, XP_053907960.1; Cuculus canoru TNFα2, XP_053907961.1; Podarcis lilfordi TNFα, CAI5768086.1; Rana temporaria TNFα, XP_040179046.1; Pelobates cultripes TNFα, CAH2314388.1; Bombina bombina TNFα, XP_053545132.1; Oncorhynchus mykiss TNFα, XP_021415456.1; Larimichthys crocea TNFα, NP_001290314.1; Salmo salar TNFα, XP_014034205.1; Sinocyclocheilus anshuiensis TNFα, XP_016327880.1; Danio rerio TNFα, AAR06286.1; Ictalurus punctatus TNFα, NP_001187101.1; Paralichthys olivaceus TNFα, BAA94969.1; Gallus gallus TNFα, AUG72034.1; Scophthalmus maximus TNFα, ACN41911.1; Epinephelus coioides TNFα1, AEH59794.1; Epinephelus coioides TNFα2, AEH59795.1; Ctenopharyngodon idella TNFα, ADY80577.1. TNFα sequences from different species were clarified by rainbow.

expressed as micromole MDA per milligram of protein. The experiment was repeated in triplicate.

2.10.7. Diamine oxidase (DAO) activity

DAO activity in midgut was measured by using a DAO assay kit (Solarbio, China). After triplicate measurements, DAO activity was calculated with absorbance changes at OD_{500} nm.

2.11. RNA isolation, cDNA synthesis and qRT-PCR assay

Based on previous studies, total RNA was isolated from above tissues and harvested cells and treated with DNAase to avoid genomic contamination by using total RNA isolation kit V2 (Vazyme Biotech, China) [37]. After RNA quality check, 1000 ng of purified total RNA was used to synthesize cDNA templates by using MonScript™ RT III All-in-One Mix with dsNase (Monad, China). Relative expression profiles of TNF α 1, Fas-associating protein with a novel death domain (FADD), caspase 7 (CASP7), caspase 3 (CASP3), caspase 8 (CASP8), heat shot protein 70 (HSP70), heat shot protein 90α (HSP90 α), heat shot protein 90β ((HSP90β), activating transcription factor 4 (ATF4), activating transcription factor 6 (ATF6), Inosital-requiring enzyme 1 (IRE1), protein disulfide isomerase family A, member 3 (PDIA3), X-box binding protein 1 (XBP1), zonula occludens-1 (ZO-1), occludin, claudin-1, claudin-3, claudin-6, and claudin-9, oxidation resistance 1 (OXR1), thioredoxin reductase (TrxR), CuZnSOD (SOD1), mucin 2 (MUC2), mucin 13 (MUC13), cytochrome c oxidase 4 (COX4), cytochrome P450 11 A (CYP11A1) and 18S rRNA were investigated by qRT-PCR assay [36]. The above primers were shown in Table 1. Additionally, qRT-PCR reaction contained: 10.0 μL SYBR Green Master Mix (ABI), 2.0 μL cDNA template, 0.5 μL each primer and 7.0 μL ddH₂O. Following confirmation by melting curve analysis, qRT-PCR results were calculated by using 2 - \triangle Ct methods [38]. The calculated results were subjected to triplicate measurements.

2.12. Statistical analyses

SPSS program was used for data calculation, which is subjected to one-way ANOVA or *t*-test analysis. GC numbers and (L/W) ratios in midgut villi were measured by using Image J software. Chart generation was executed by using Origin software. Whist the analytical levels reach <0.05 *P*-value, results were statistically significant.

3. Results

3.1. Characterization of TNF α 1 sequences

The nucleotide and amino acid sequences of WCC-TNF α 1 were shown in supplementary Fig. 1. The ORF sequence of WCC-TNF α 1 encoded a polypeptide of 232 amino acid residues with an estimated molecular mass of 25.66 KDa and a predicted isoelectronic point of 6.83. In Fig. 1A, a transmembrane region, a TNF domain, seven trimer interface sites (H⁸⁴F¹²⁹Y¹³¹Y¹⁹³F¹⁹⁸F²²⁶F²³⁰) and six receptor binding sites (R¹⁰¹K¹⁰²A¹⁰⁷S¹⁵⁴S¹⁶¹S¹⁶⁶) were analyzed in the structure of WCC-TNF α 1. In Fig. 1B, secondary structure of WCC-TNF α 1 possessed 3 sheets, 3 β -hairpins, 3 β -bulges, 11 strands and 1 disulphide. In Fig. 1C, tertiary structure of WCC-TNF α 1 was 70 % identical to c7dovB template

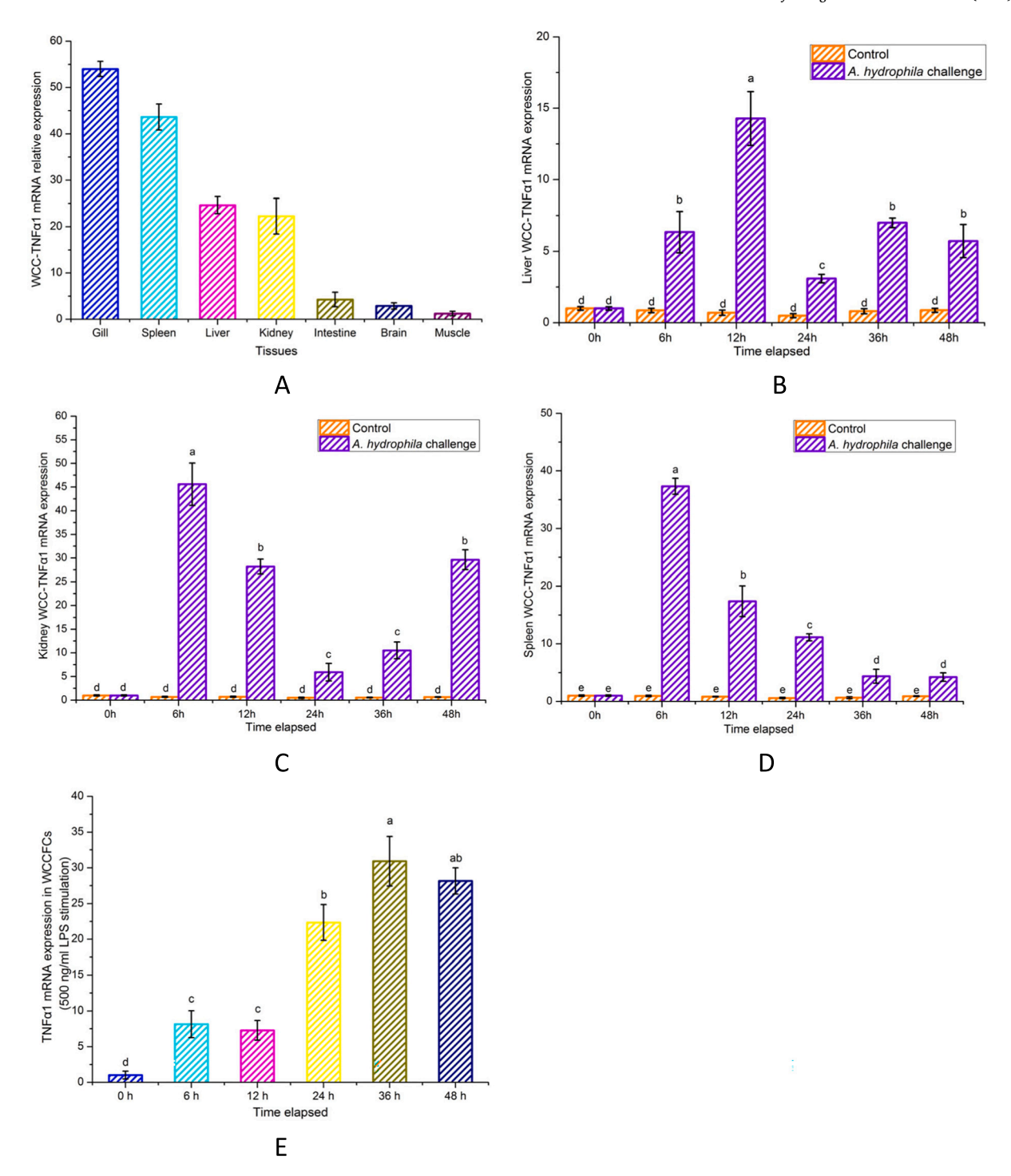


Fig. 3. Gene expression levels of WCC-TNF α 1. (A) Tissue-specific expressions determined by qRT-PCR assay. (B—D) Expressions of WCC-TNF α 1 were detected in liver, kidney and spleen at 0, 6, 12, 24, 36 and 48 h post-challenge. (E) Expression levels of TNF α 1 in WCCFCs subjected to LPS exposure. The calculated data (mean \pm SD) with different letters were significantly different (P < 0.05) among the groups. The experiments were performed in triplicate.

modeled with exceeding a 95 % confidence. In Fig. 1D, tertiary structure of WCC-TNF α 1 possessed 10 predominant clefts, only two clefts marked in red and purple contained the maximum volumes of 3136.64 A^3 and 3240.32 A^3, respectively. In Fig. 2, phylogenetic analysis implied that TNF α showed a high evolutionary conservatism among species. Fish TNF α sequences are predominately divided into two branches and WCC-TNF α 1 sequence exhibited a close similarity to the counterparts of other freshwater teleost fish.

3.2. Expression profiles of TNF α 1

In Fig. 3A, tissue-specific expression analysis revealed that the highest expression level of WCC-TNF α 1 was detected in gill, followed by spleen, liver and kidney, whereas low-level expression of WCC-TNF α 1 mRNA was observed in muscle. In Fig. 3B, WCC-TNF α 1 expression significantly increased from 6 h to 12 h and achieved the highest level at 12 h after *A. hydrophila* challenge (P < 0.05), followed by a sharp decline from 24 h to 48 h. In Fig. 3C, fish receiving *A. hydrophila* infection showed a upregulated profiles of WCC-TNF α 1 expression in kidney with

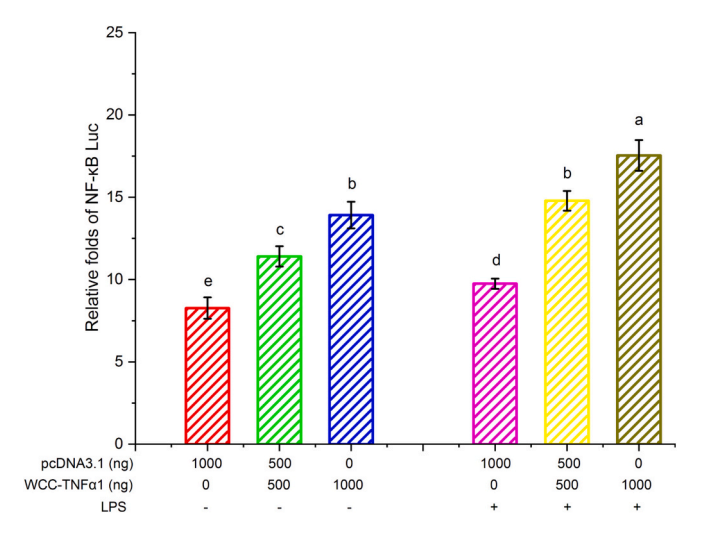


Fig. 4. Effect of WCC-TNF α 1 overexpression on the promoter activities. Cells were co-transfected with PRL-TK, NF- κ B Luc, together with pcDNA3.1 or pcDNA3.1-WCC-TNF α 1. The calculated data (mean \pm SD) with different letters were significantly different (P < 0.05). The experiments were performed in triplicate.

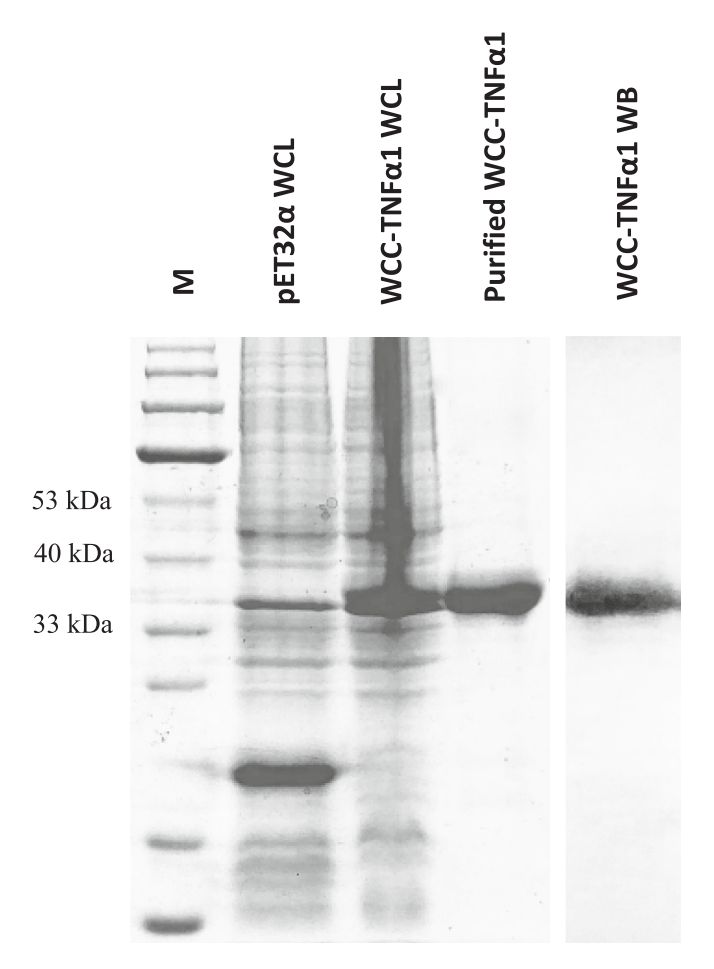


Fig. 5. Generation and validation of TNFα1 fusion proteins. Lane M: protein molecular standard; Lane pET32α WCL: total protein was isolated from lysis of pET32α-BL21 after IPTG induction; Lane WCC-TNFα1 WCL: total protein was isolated from lysis of pET32α-WCC-TNFα1-BL21 after IPTG induction; Lane purified WCC-TNFα1: WCC-TNFα1 fusion protein was purified by using Ni-NTA; Lane WCC-TNFα1 WB: purified fusion protein was identified by using anti-His tag antibody.

peaked level at 6 h (P < 0.05). In Fig. 3D, splenic WCC-TNF α 1 mRNA expression attained the peaked value at 6 h after A. hydrophila challenge (P < 0.05), followed by a gradual decrease from 6 h to 36 h. In Fig. 3E, WCC-TNF α 1 mRNA began to increase at 6 h and gradually attained the peaked expression at 24 h in WCCFCs after 500 ng/mL LPS exposure (P < 0.05).

3.3. WCC-TNFa1 overexpression promote NF-κB activation in WCCFCs

As shown in Fig. 4, WCC-TNF α 1 overexpression could significantly elevate NF- κ B luciferase activity in WCCFCs. 500 ng WCC-TNF α 1 plasmid could enhance NF- κ B luciferase activity to 1.38-fold by comparing with that of control vector group (P < 0.05), whereas 1000 ng WCC-TNF α 1 plasmid could achieve 1.68-fold increase in NF- κ B activity by comparing with that of control vector group (P < 0.05).

Furthermore, LPS stimulation could augment TNF α 1-induced NF- κ B activity in WCCFCs. Overexpression of 500 ng WCC-TNF α 1 plasmid can reach 1.52-fold increase of NF- κ B activity in WCCFCs exposed to LPS stimulation by comparing with that of control vector group (P<0.05), whereas 1000 ng WCC-TNF α 1 plasmid overexpression could enhance NF- κ B luciferase activity to 1.81-fold by comparing with that of control vector group (P<0.05).

3.4. Prokaryotic expression and fusion protein validation

In Fig. 5, a clear IPTG-induced fusion protein of approximately 36.0 KDa was detected in pET32a-WCC-TNF α 1 transformed cells, while no significant elevation of IPTG-induced protein was detected in pET32a transformed cells. After Ni-NTA purification, the purified TNF α 1 fusion proteins were confirmed by western blotting using anti-His antibody.

3.5. Effect of TNF α 1 stimulation on histological changes in midgut

In Fig. 6A-B, WCC receiving anal intubation with WCC-TNFα1 showed a fuzzy appearance of brush broader in impaired villi along with vacuolization and edema of midgut wall by comparing with that of the control. In Fig. 6C-D, WCC-TNFα1 treatment could cause atrophic GC changes in midgut villi. The average GC numbers showed a 3.62-fold decrease in villi of WCC-TNFa1 treated midgut by comparing with the control (P < 0.05), while no significant difference of L/W ratio was observed among the groups. In Fig. 6E, DAO is a key injury marker of epithelial integrity of the intestinal mucosa. WCC-TNFα1 treatment could significantly increase DAO activity in midgut and a 4.16-fold elevation of DAO activity was observed in midgut of WCC following TNF α 1 stimulation in comparison with the control (P < 0.05). As shown in Fig. 6F, a 3.97-, 1.30-, 1.56-, 1.48-, 1.42-, 1.67-, 2.51- and 2.03-fold decrease of ZO-1, occludin, claudin 1, claudin 3, claudin 6, claudin 9, MUC2 and MUC13 was detected in midgut treated with WCC-TNFα1 by comparing with the control (P < 0.05), suggesting that WCC-TNF α 1 treatment may impair tight junction integrity and alleviate mucosal immunity in gut epithelium.

3.6. Effect of $TNF\alpha 1$ stimulation on immune-related gene expression in midgut

The immune-related genes involved in TNF signals and redox balance were investigated. As shown in Fig. 7A, relative expressions of FADD, CASP3, CASP7, CASP8, ATF4, ATF6, IRE1, PDIA3 and XBP1 in TNF α 1-treated midgut were approximately 3.71-, 2.77-, 3.43-, 3.96-, 4.21-, 3.48-, 2.68-, 5.03- and 3.03-fold higher than those of the control (P < 0.05). In Fig. 7B, relative expressions of HSP70, HSP90 α , HSP90 β , OXR1, TxR and TXNL decreased sharply in midgut following WCC-TNF α 1 treatment, while 6.96- and 4.11-fold increased levels of COX4 and CYP11A1 were monitored.

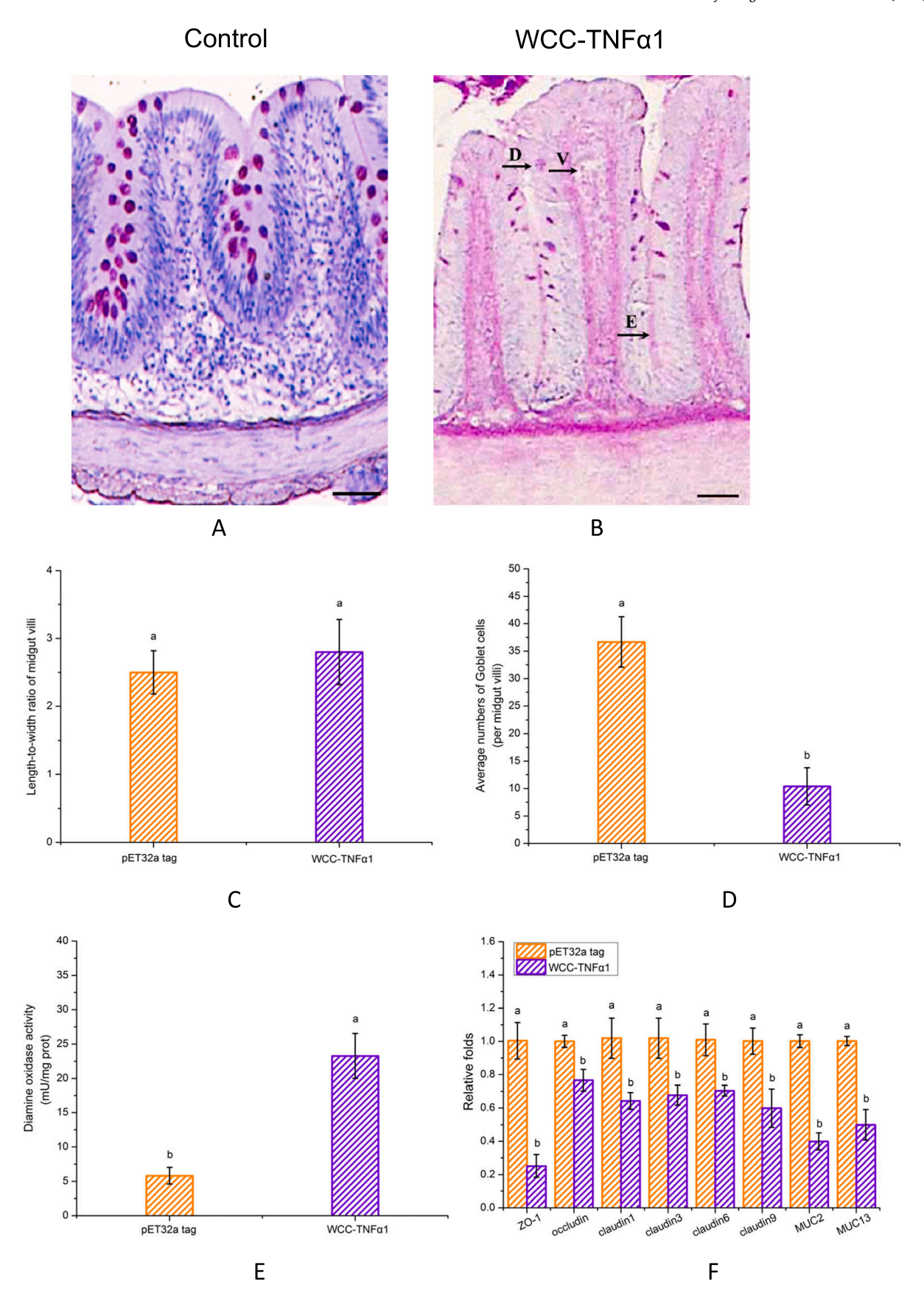


Fig. 6. Histological analysis in midgut by $In\ vivo$ administration of WCC-TNF α 1 fusion protein. (A-B) Midgut tissues were sectioned and stained by using PAS staining kit. D: villi deformation; F: villus fusion; E: edema of midgut wall. Villus length-to-width (L/W) ratios (C), average numbers of goblet cells (D) and midgut DAO activities (E) were determined. (F) Expressions of TJ genes and mucins in midgut perfused with WCC-TNF α 1. The calculated data (mean \pm SD) with different letters were significantly different (P < 0.05) among the groups. The experiments were performed in triplicate.

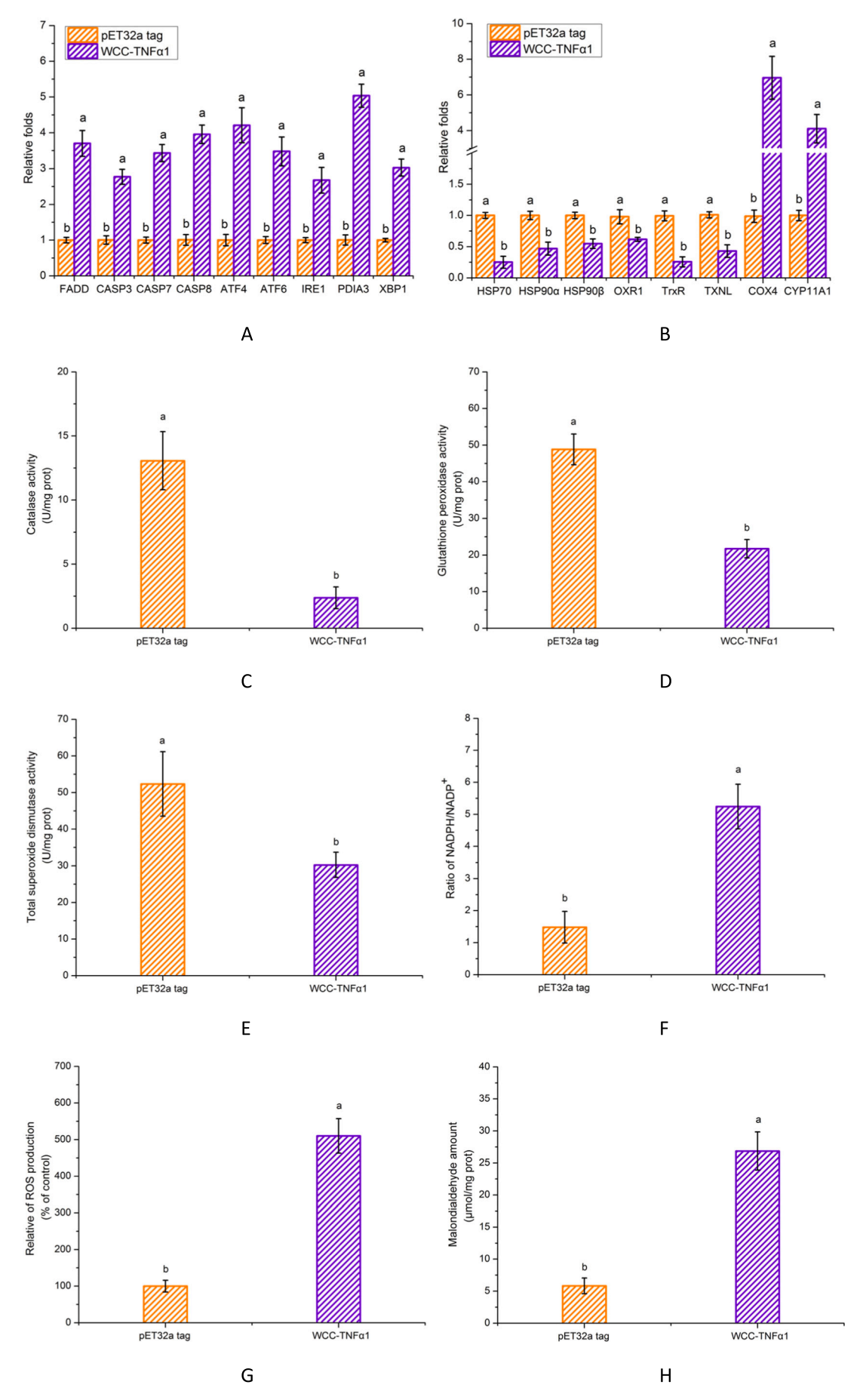


Fig. 7. In vivo administration of WCC-TNFα1 fusion protein regulated immune response in midgut. (A) Expressions of apoptosis genes and UPR genes in midgut perfused with WCC-TNFα1. (B) Expressions of antioxidant genes and redox responsive genes in midgut perfused with WCC-TNFα1. (C-E) Analyses of CAT, GPx and total SOD were detected in midgut. (F—H) NADPH/NADP $^+$ ratio, relative ROS production and MDA amount were determined in midgut. The calculated data (mean \pm SD) with different letters were significantly different (P < 0.05) among the groups. The experiments were performed in triplicate.

3.7. Measurement of antioxidant status in midgut

In Fig. 7C-E, fish receiving WCC-TNF α 1 stimulation showed a 5.49-, 2.24- and 1.73-fold reduction of CAT activity, GPx activity and total SOD activity in midgut by comparing with those of the control (P < 0.05). As shown in Fig. 7F-H, NADPH/NADP⁺ ratio, ROS content and MDA amount in WCC-TNF α 1 group were approximately 3.54-, 5.10- and 4.62-fold higher than those of the control groups (P < 0.05).

4. Discussion

In this study, TNF α 1 gene was identified in WCC. The deduced WCC-TNF α 1 amino acid sequence contained three high-conserved motifs: a TNF domain, seven trimer interface sites and six receptor binding sites. Previous findings demonstrated that the compact jellyroll folding generated by trimer interface sites and receptor binding subunits in TNF α structure may play a pivotal role in efficient signal transduction of TNF pathways [39]. Thus, we speculated that WCC-TNF α 1 may play a functionally conserved role in signal pathways. qRT-PCR analysis revealed that WCC-TNF α 1 was expressed in a wide range of isolated tissues with a high-expressed level in gill. Elevated trends of WCC-TNF α 1 expressions were observed in immune-related tissues and cultured cells upon *in vitro* stimulation, suggesting that WCC-TNF α 1 may play an important role in immune regulation. However, the regulatory role of WCC-TNF α 1 in gut immunity of fish is unclear.

In general, tight junction constitutes a physiological barrier that can elicit the first line of host innate immune defense against invading pathogens in environment [40]. Furthermore, gut epithelial cells acting as important sensors can directly recognize invading microbes and enable the chemoattraction of activated immune cells to adhere to gut surfaces [41]. GCs distribution and mucus function can enable the secretion of mucin glycoproteins and bioactive molecules to promote immune cell connection and orchestrate mucosal immune response to invasive pathogens [42,43]. ZO-1, occludin, claudin 1, claudin 3, claudin 6, claudin 9 are the important TJ genes in gut epithelial cells, while MUC2 and MUC13 are key mucin glycans participating in mucosal immunity [44]. Gut injury is usually accompanied by villus deformation and increased levels of DAO index, which were the two predominant pathological indicators that can reflect the injured degrees of mucosal immunity in gut tract [45]. In this study, WCC receiving WCC-TNFα1 perfusion exhibited a severe pathological changes in impaired midgut, along with GC decrease and DAO elevation. Moreover, expression profiles of ZO-1, occludin, claudin 1, claudin 3, claudin 6, claudin 9, MUC2 and MUC13 reduced significantly in midgut of WCC upon stimulation. These results suggested that WCC-TNFα1 treatment could significantly promote epithelial permeability enhance midgut injury in WCC.

TNF α is a proinflammatory cytokine belonging to TNF superfamily, which can induce the recruitment of adaptor molecule FADD via TNF α receptor [46]. FADD, a pivotal component in cell death signals, can enable the synchronization between active TNF α receptors and CASP molecules (CASP3, CASP7 and CASP8) via NF- κ B pathway, which is able to determine the choice between cell life or death events [47]. Current study suggested that WCC-TNF α 1 overexpression could dramatically increase NF- κ B activity in WCCFCs with or without LPS stimulation. Death receptor-mediated extrinsic apoptosis and necroptosis are highly modulated cell death process that can boost immunological tolerance,

maintain host homeostasis as well as remodel inflammatory response in impaired tissues [48,49]. In addition, ROS stimulation by $TNF\alpha$ or oxidants can orchestrate the synergy between innate immunity and adaptive immune response, but its long-term increase can hamper normal function of macromolecular properties, including ROS overproduction and lipid peroxidation, and promote cell death via caspase signals [50,51]. NADPH is required by enzymes involved in pathogenesis of metabolic disorder and high ratio of NADPH/NADP⁺ is correlated with increased level of oxidative stress [52]. In contrast, antioxidant enzymes and endogenous antioxidants, including OXR1, TXNL, TrxR, SOD, GPx and CAT, are playing a frontline role in antioxidant response to in vitro stimuli [53]. HSP70, HSP90α and HSP90β are high-conserved chaperones as the crucial stress sensors participating in a variety of cellular processes such as protein folding, degradation and translocation [54,55]. However, continuous accumulation of free radical in gut tract can exacerbate the disruption of cellular homeostasis, cause emerging production of misfolded proteins in endoplasmic reticulum as well disturb redox-dependent protein folding process [56,57]. As is well known, AT4, ATF6, IRE1, PDIA3 and XBP1 were the crucial regulators involved in three signal pathways of unfolded protein response (UPR), including IRE1α-XBP1 pathway, PERK pathway and ATF6 pathway [58]. UPR is an integrated signal pathway that can alleviate the biosynthetic burden and cope with the stress imperiling all living cells [59]. UPR activation exhibits a cytoprotective effect on homeostasis restoration in tissues or cells suffering from deleterious stressors and severe illness, while its subversion may aggravate immune insult [60]. In this study, WCC-TNFα1 perfusion could alleviate expression profiles of HSP70, HSP90α, HSP90β, OXR1, TrxR and TXNL in midgut of WCC, while the expressions of apoptotic genes, UPR genes and redox responsive genes increased sharply. In addition, enzymatic activity of CAT, GPx and total SOD decreased significantly in TNFα1-perfused midgut, along with increased levels of NADPH/NADP+ ratios, ROS production and MDA amount. These results indicated that ROS-induced cytotoxic stress was involved in antioxidant insult and apoptotic process in TNFα1-treated midgut of WCC via NF-κB pathway.

In summary, WCC-TNF α 1 architecture was firstly characterized in this study. Then, expression profiles of WCC-TNF α 1 in healthy WCC, A. hydrophila-infected WCC and LPS-stimulated cells were measured, respectively. WCC-TNF α 1 perfusion could dramatically attenuate TJ gene expressions and reduce GC numbers in midgut of WCC. In addition, a dramatic decrease of antioxidant status was observed in WCC-TNF α 1 treated midgut, along with elevated levels of apoptotic processes. Our results revealed that WCC-TNF α 1 cytotoxicity may cause antioxidant insults and facilitate the mucosal immune damage in midgut of WCC.

Supplementary data to this article can be found online at $\frac{\text{https:}}{\text{doi.}}$ org/10.1016/j.ijbiomac.2023.127770.

CRediT authorship contribution statement

Shi-Yun Li and Ning-Xia Xiong performed methodology and formal analysis; Ke-Xin Li, Jin-Fang Huang, Jie Ou and Fei Wang performed verification; Ming-Zhu Huang performed conceptualization; Sheng-Wei Luo performed conceptualization, supervision, project management and article writing.

Funding

This research was supported by the National Natural Science Foundation of China, China (grant no. 31902363), Hunan Provincial Natural Science Foundation of China, China (grant no. 2021JJ40340).

Declaration of competing interest

The authors declare that they have no conflict of interest.

References

- D. Bucke, Aquatic pollution: effects on the health of fish and shellfish, Parasitology 106 (1993) S25–S37.
- [2] B. Austin, The effects of pollution on fish health, J. Appl. Microbiol. 85 (1998) 234S-242S.
- [3] H. Dong, Y. Chen, J. Wang, Y. Zhang, P. Zhang, X. Li, et al., Interactions of microplastics and antibiotic resistance genes and their effects on the aquaculture environments, J. Hazard. Mater. 403 (2020), 123961.
- [4] S.A. Kraemer, A. Ramachandran, G.G. Perron, Antibiotic pollution in the environment: from microbial ecology to public policy, Microorganisms 7 (2019)
- [5] H.D. Rodger, Fish disease causing economic impact in global aquaculture, in: Fish Vaccines, Springer, 2016, pp. 1–34.
- [6] S. Boltaña, N. Roher, F.W. Goetz, S.A. MacKenzie, PAMPs, PRRs and the genomics of gram negative bacterial recognition in fish, Dev. Comp. Immunol. 35 (2011) 1195–1203.
- [7] Z. Lian, J. Bai, X. Hu, A. Lü, J. Sun, Y. Guo, et al., Detection and characterization of Aeromonas salmonicida subsp. salmonicida infection in crucian carp Carassius auratus, Vet. Res. Commun. 44 (2020) 61–72.
- [8] S.T. Oliveira, G. Veneroni-Gouveia, M.M. Costa, Molecular characterization of virulence factors in Aeromonas hydrophila obtained from fish, Pesquisa Veterinária Brasileira 32 (2012) 701–706.
- [9] F. Wang, Z.L. Qin, W.S. Luo, N.X. Xiong, M.Z. Huang, J. Ou, et al., Alteration of synergistic immune response in gut-liver axis of white crucian carp (Carassius cuvieri) after gut infection with Aeromonas hydrophila, J. Fish Dis. 00 (2023) 1–11.
- [10] B. Magnadottir, Immunological control of fish diseases, Marine Biotechnol. 12 (2010) 361–379
- [11] J.B. Jørgensen, The innate immune response in fish, Fish Vaccination 1 (2014) 84-102.
- [12] N.-X. Xiong, W.-S. Luo, X.-Y. Kuang, F. Wang, Z.-X. Fang, J. Ou, et al., Gut-liver immune and redox response in hybrid fish (Carassius cuvieri♀× Carassius auratus red var.♂) after gut infection with Aeromonas hydrophila, Comp. Biochem. Physiol. Part C: Toxicol. Pharmacol. 266 (2023), 109553.
- [13] Z. Miao, Z. Miao, X. Teng, S. Xu, Melatonin alleviates lead-induced fatty liver in the common carps (Cyprinus carpio) via gut-liver axis, Environ. Pollut. 317 (2023), 120730.
- [14] I. Salinas, The mucosal immune system of teleost fish, Biology 4 (2015) 525–539.
- [15] S. Torrecillas, D. Montero, M.J. Caballero, K.A. Pittman, M. Custódio, A. Campo, et al., Dietary mannan oligosaccharides: counteracting the side effects of soybean meal oil inclusion on European sea bass (Dicentrarchus labrax) gut health and skin mucosa mucus production? Front. Immunol. 6 (2015) 397.
- [16] Y. Deng, Y. Zhang, H. Chen, L. Xu, Q. Wang, J. Feng, Gut-liver immune response and gut microbiota profiling reveal the pathogenic mechanisms of vibrio harveyi in pearl gentian grouper (*Epinephelus lanceolatus3* × *E. fuscoguttatus*\$\(\text{Q}\), Front. Immunol. 11 (2020) 607754.
- [17] N. Wu, Y.-L. Song, B. Wang, X.-Y. Zhang, X.-J. Zhang, Y.-L. Wang, et al., Fish gut-liver immunity during homeostasis or inflammation revealed by integrative transcriptome and proteome studies, Sci. Rep. 6 (2016) 1–17.
- [18] J. Shan, G. Wang, H. Li, X. Zhao, W. Ye, L. Su, et al., The immunoregulatory role of fish specific type II SOCS via inhibiting metaflammation in the gut-liver axis, Water Biol. Security 2 (2023), 100131.
- [19] H. Himmerich, A.J. Sheldrick, TNF-α and ghrelin: opposite effects on immune system, metabolism and mental health, Protein Pept. Lett. 17 (2010) 186–196.
- [20] Y. Li, T. Xiao, J. Zou, Fish TNF and TNF receptors, Sci. China Life Sci. 64 (2021) 196–220.
- [21] S. Kinoshita, G. Biswas, T. Kono, J. Hikima, M. Sakai, Presence of two tumor necrosis factor (tnf)-α homologs on different chromosomes of zebrafish (Danio rerio) and medaka (Oryzias latipes), Mar. Genomics 13 (2014) 1–9.
- [22] M. Huang, P. Mu, X. Li, Q. Ren, X.-Y. Zhang, Y. Mu, et al., Functions of TNF- α 1 and TNF- α 2 in large yellow croaker (Larimichthys crocea) in monocyte/macrophage activation, Dev. Comp. Immunol. 105 (2020), 103576.
- [23] S. Hong, R. Li, Q. Xu, C.J. Secombes, T. Wang, Two types of TNF-α exist in teleost fish: phylogeny, expression, and bioactivity analysis of type-II TNF-α3 in rainbow trout Oncorhynchus mykiss, J. Immunol. 191 (2013) 5959–5972.

- [24] K. Li, H. Qiu, J. Yan, X. Shen, X. Wei, M. Duan, et al., The involvement of TNF-α and TNF-β as proinflammatory cytokines in lymphocyte-mediated adaptive immunity of Nile tilapia by initiating apoptosis, Dev. Comp. Immunol. 115 (2021), 103884
- [25] F. Wang, Z.-L. Qin, W.-S. Luo, N.-X. Xiong, S.-W. Luo, Aeromonas hydrophila can modulate synchronization of immune response in gut-liver axis of red crucian carp via the breach of gut barrier, Aquac. Int. (2023) 1–15.
- [26] N.-X. Xiong, Z.-X. Fang, X.-Y. Kuang, J. Ou, S.-W. Luo, S.-J. Liu, Integrated analysis of gene expressions and metabolite features unravel immunometabolic interplay in hybrid fish (Carassius cuvieri

 Varassius auratus red vara) infected with Aeromonas hydrophila, Aquaculture 563 (2023), 738981.
- [27] S.-W. Luo, Z.-W. Mao, Z.-Y. Luo, N.-X. Xiong, K.-K. Luo, S.-J. Liu, et al., Chimeric ferritin H in hybrid crucian carp exhibit a similar down-regulation in lipopolysaccharide-induced NF-κB inflammatory signal in comparison with Carassius cuvieri and Carassius auratus red var, Comp. Biochem. Physiol. C Toxicol. Pharmacol. (2021) 108966.
- [28] C. Fierro-Castro, L. Barrioluengo, P. López-Fierro, B. Razquin, A. Villena, Fish cell cultures as in vitro models of inflammatory responses elicited by immunostimulants. Expression of regulatory genes of the innate immune response, Fish Shellfish Immunol. 35 (2013) 979–987.
- [29] Z.-H. Qi, Y.-F. Liu, S.-W. Luo, C.-X. Chen, Y. Liu, W.-N. Wang, Molecular cloning, characterization and expression analysis of tumor suppressor protein p53 from orange-spotted grouper, Epinephelus coioides in response to temperature stress, Fish Shellfish Immunol. 35 (2013) 1466–1476.
- [30] C. Yang, S. Yang, Y. Miao, J. Shu, Y. Peng, J. Li, et al., PRMT6 inhibits K63-linked ubiquitination and promotes the degradation of IRF3 in the antiviral innate immunity of black carp Mylopharyngodon piceus, Aquaculture 562 (2023), 738872.
- [31] N.-X. Xiong, J. Ou, S.-Y. Li, J.-H. Zhao, J.-F. Huang, K.-X. Li, et al., A novel ferritin L (FerL) in hybrid crucian carp could participate in host defense against Aeromonas hydrophila infection and diminish inflammatory signals, Fish Shellfish Immunol. 120 (2022) 620–632.
- [32] J. Fu, Y. Huang, J. Cai, S. Wei, Z. Ouyang, F. Ye, et al., Identification and characterization of Rab7 from orange-spotted grouper, *Epinephelus coioides*, Fish Shellfish Immunol. 36 (2014) 19–26.
- [33] G.-H. Cha, S.-W. Luo, Z.-h. Qi, Y. Liu, W.-N. Wang, Optimal conditions for expressing a complement component 3b functional fragment (α2-macroglobulin receptor) gene from Epinephelus coioides in Pichia pastoris, Protein Expr. Purif. 109 (2015) 23–28.
- [34] N.-X. Xiong, F. Wang, W.-S. Luo, J. Ou, Z.-L. Qin, M.-Z. Huang, et al., Tumor necrosis factor α2 (TNFα2) facilitates gut barrier breach by Aeromonas hydrophila and exacerbates liver injury in hybrid fish, Aquaculture 577 (2023), 739995.
- [35] M.K. Jeong, B.-H. Kim, Grading criteria of histopathological evaluation in BCOP assay by various staining methods, Toxicol. Res. 38 (2022) 9–17.
- [36] C.-H. Cheng, Y.-L. Su, H.-L. Ma, Y.-Q. Deng, J. Feng, X.-L. Chen, et al., Effect of nitrite exposure on oxidative stress, DNA damage and apoptosis in mud crab (Scylla paramamosain), Chemosphere 239 (2020), 124668.
- [37] L. Fan, G. Liao, Z. Wang, H. Liu, K. Cheng, J. Hu, et al., Insight into three water additives: revealing the protective effects on survival and stress response under cold stress for Pacific white shrimp Litopenaeus vannamei, Fish Shellfish Immunol. 139 (2023), 108845.
- [38] K.J. Livak, T.D. Schmittgen, Analysis of relative gene expression data using real-time quantitative PCR and the $2-\Delta\Delta$ CT method, methods 25 (2001) 402–408.
- [39] É.S. Vanamee, D.L. Faustman, Structural principles of tumor necrosis factor superfamily signaling, Sci. Signal. 11 (2018) eaao4910.
- [40] E.E. Schneeberger, R.D. Lynch, The tight junction: a multifunctional complex, Am. J. Phys. Cell Phys. 286 (2004) C1213–C1228.
- [41] M.F. Kagnoff, L. Eckmann, Epithelial cells as sensors for microbial infection, J. Clin. Invest. 100 (1997) 6–10.
- [42] Y.S. Kim, S.B. Ho, Intestinal goblet cells and mucins in health and disease: recent insights and progress, Curr. Gastroenterol. Rep. 12 (2010) 319–330.
- [43] T. Pelaseyed, J.H. Bergström, J.K. Gustafsson, A. Ermund, G.M. Birchenough, A. Schütte, et al., The mucus and mucins of the goblet cells and enterocytes provide the first defense line of the gastrointestinal tract and interact with the immune system, Immunol. Rev. 260 (2014) 8–20.
- [44] K. Robinson, Z. Deng, Y. Hou, G. Zhang, Regulation of the intestinal barrier function by host defense peptides, Front. Vet. Sci. 2 (2015) 57.
- [45] J.-j. Zhang, J.-q. Wang, X.-y. Xu, J.-y. Yang, Z. Wang, S. Jiang, et al., Red ginseng protects against cisplatin-induced intestinal toxicity by inhibiting apoptosis and autophagy via the PI3K/AKT and MAPK signaling pathways, Food Funct. 11 (2020) 4236–4248.
- [46] B. Beutler, C. Van Huffel, Unraveling function in the TNF ligand and receptor families, Science 264 (1994) 667–668.
- [47] L. Tourneur, G. Chiocchia, FADD: a regulator of life and death, Trends Immunol. 31 (2010) 260–269.
- [48] M. Chen, Y.-H. Wang, Y. Wang, L. Huang, H. Sandoval, Y.-J. Liu, et al., Dendritic cell apoptosis in the maintenance of immune tolerance, Science 311 (2006) 1160–1164.
- [49] H.-B. Shu, D.R. Halpin, D.V. Goeddel, Casper is a FADD-and caspase-related inducer of apoptosis, Immunity 6 (1997) 751–763.

- [50] K. Kaur, A.K. Sharma, S. Dhingra, P.K. Singal, Interplay of TNF- α and IL-10 in regulating oxidative stress in isolated adult cardiac myocytes, J. Mol. Cell. Cardiol. 41 (2006) 1023–1030.
- [51] S. Rizwan, P. ReddySekhar, B. MalikAsrar, Reactive oxygen species in inflammation and tissue injury, Antioxid. Redox Signal. 20 (2014) 1126–1167.
- [52] S. Mejía, L. Gutman, C. Camarillo, R. Navarro, M. Becerra, L. Santana, M. Cruz, E. Pérez, M. Flores, Nicotinamide prevents sweet beverage-induced hepatic steatosis in rats by regulating the G6PD, NADPH/NADP+ and GSH/GSSG ratios and reducing oxidative and inflammatory stress, Eur. J. Pharmacol. 818 (2018) 499–507.
- [53] A. Sahreen, K. Fatima, T. Zainab, M.K. Saifullah, Changes in the level of oxidative stress markers in Indian catfish (Wallago attu) infected with Isoparorchis hypselobagri, Beni-Suef Univ. J. Basic Appl. Sci. 10 (2021) 1–8.
- [54] E. Padmini, Rani M. Usha, Heat-shock protein 90 alpha (HSP90α) modulates signaling pathways towards tolerance of oxidative stress and enhanced survival of hepatocytes of Mugil cephalus, Cell Stress and Chaperones 16 (2011) 411–425.

- [55] M.A. Yenari, J. Liu, Z. Zheng, Z.S. Vexler, J.E. Lee, R.G. Giffard, Antiapoptotic and anti-inflammatory mechanisms of heat-shock protein protection, Ann. N. Y. Acad. Sci. 1053 (2005) 74–83.
- [56] A. Bhattacharyya, R. Chattopadhyay, S. Mitra, S.E. Crowe, Oxidative stress: an essential factor in the pathogenesis of gastrointestinal mucosal diseases, Physiol. Rev. 94 (2014) 329–354.
- [57] W.C. Chong, M.D. Shastri, R. Eri, Endoplasmic reticulum stress and oxidative stress: a vicious nexus implicated in bowel disease pathophysiology, Int. J. Mol. Sci. 18 (2017) 771.
- [58] A.W. Chuang, O. Kepp, G. Kroemer, L. Bezu, Endoplasmic reticulum stress in the cellular release of damage-associated molecular patterns, Int. Rev. Cell Mol. Biol. 350 (2020) 1–28.
- [59] C.Y. Liu, R.J. Kaufman, The unfolded protein response, J. Cell Sci. 116 (2003) 1861–1862.
- [60] J. Celli, R.M. Tsolis, Bacteria, the endoplasmic reticulum and the unfolded protein response: friends or foes? Nat. Rev. Microbiol. 13 (2015) 71–82.